Design and implementation details of a low cost sensorless emulator for variable speed wind turbines

Soufyane Benzaouia, Mohammed Mokhtari, Smail Zouggar, Abdelhamid Rabhi, Mohamed Larbi Elhafyani, Taoufik Ouchbel

Version of Record: https://www.sciencedirect.com/science/article/pii/S2352467721000023
Manuscript_ed5b6a7ac67434e114fecb8fbed731c3

Design and Implementation Details of a Low Cost Sensorless Emulator for Variable Speed Wind Turbines

Benzaouia Soufyane[1,2], Mokhtari Mohammed[1], Zouggar Smail[1], Rabhi Abdelhamid[2], Elhafyani Mohamed Larbi[1], Ouchbel Taoufik[1]

[1] Laboratory of Electrical Engineering and Maintenance – LEEM, University Mohammed 1st, High School of Technology Oujda, Morocco

[2] Laboratory of Modelisation, Information and Systems – MIS, University of Picardie Jules Verne, 33 rue Saint Leu, 80039 Amiens Cedex, France

soufyane.benzaouia@gmail.com

Abstract *- In this paper, a low cost wind turbine emulator (WTE) is designed and implemented. The aim is accurately simulating the nonlinear behaviors and characteristics of a real wind turbine. It is well known that each wind turbine has its own power coefficient characteristic. This work contains an analysis of the WTE by considering the main power coefficient models known in literature. Speed sensor is one of the most important component used to provide the shaft speed information. This latter will increase greatly the system cost and volume of the control scheme. In our work, we propose cheapest solution by using a second-order sliding-mode speed observer based on super-twisting algorithm. Note that the accurate speed estimation is essential to maintain good simulation of wind turbine characteristics. The WTE closed loop operation is ensured by the fuzzy logic technique. Experimental results confirm the effectiveness of the proposed sensorless WTE solution.*

Keywords: *Wind turbine emulator, DC motor, Second-order sliding-mode speed observer, Fuzzy logic control, Power coefficient.*

I. INTRODUCTION

Recently and like all renewable energies kinds, wind energy is experiencing remarkable development [1]. A lot of research has been done on this field [2][3]. A test bench environment is required for validating and improving the wind turbines control. It is known that wind turbines have a non-linear behavior. A wind turbine emulator (*WTE*) is an important equipment used for simulating the static, dynamic and the nonlinear characteristics of a real wind turbine without depending on natural wind resource and commercialized wind turbines [4][5][6].

In literature, several wind turbine emulators have been designed and realized. The *WTE* is built by coupling the generator shaft to a motor called prime mover, this latter is controlled using a variable speed drive. Three main prime movers type have been considered in different works. The first one is a *DC* motor; the second one is a permanent magnet synchronous motor (*PMSM*) and the third one is using an induction motor (*IM*). It is possible to generate the same static and dynamic characteristics as a real wind turbine by controlling the prime mover. In [7], the authors propose a *WTE* using a *DC* motor able to simulate the turbine power curves in open loop mode without using a closed loop control. In [8], the authors present a wind turbine emulator prototype based on *DC* motor as a prime mover controlled through a single-phase half-controlled drive using a *PID* controller. In [9], a wind turbine emulator is made up of *DC* motor and three-phase thyristor converter; the prime mover here is controlled using a *PI* regulator with forward compensation control in order to regulate the terminal voltage of the separately excited *DC* motor. The same prime mover associated with an *AC/DC* converter was used in [10] to accurately reproduce the turbine torque as function of shaft speed wind turbine characteristics. The same configuration has been studied in [11] and [12]. In other works, instead of using a controlled *AC/DC* converter, the *DC* motor is controlled via a *DC-DC* converter. In [13], [14], [15] and [16], a wind turbine emulator is constructed by using a *DC* power source, a *DC-DC* boost converter and a *DC* motor, the armature current is regulated to its reference using a proportional integral (*PI*) controller. The second *WTE* configurations found in literature are based on permanent-magnet synchronous motor (*PMSM*). In [17] and [18], the authors have selected a *PMSM* to implement the emulation. A field oriented control (*FOC*) based on proportional integral (*PI*) controllers was implemented for the motor control. Another wind turbine emulator based on the load torque dynamic compensation of the permanent-magnet synchronous motor (*PMSM*) is proposed in [19]. The third motor type used for building a wind turbine emulator is the induction motor (*IM*). In [20], a novel wind turbine simulator has been developed in order to design, evaluate and test an actual wind turbine, the prime mover in this work is controlled through an *IGBT* inverter. Similarly in [21], a platform composed of two coupled squirrel-cage induction machines (IM) has been developed for emulating the static and dynamic behavior of real wind energy conversion system. The implemented wind turbine emulator is used later to compare the different *MPPT* control strategies. A wind turbine simulator consisting of an induction motor driven by a torque control inverter has been developed in [22].

In this paper, a direct-current (*DC*) motor is selected to realize the wind turbine emulator. This choice according to [4] and [11] is the best, it has the advantage of being simple from the point of view control and implementation. Approximately, in most of the above-mentioned wind turbine emulators, a speed or torque sensor is used to provide the rotational speed or the mechanical torque information. The best alternative of using such mechanical sensor is to replace it by an observer or an estimator. In our work, we propose a second-order sliding-mode speed observer based on super-twisting algorithm for estimating the rotational speed of direct current motors. The proposed **sliding second-order based on super twisting algorithm** *(STA-SMO)* observer uses as input only single current and single voltage sensors. The closed loop operation of the wind turbine emulator is ensured by using the fuzzy logic technique in order to provide high convergence and stability performance during transient and steady state regime. With the designed wind turbine emulator, the main technical contributions are summarized in Table 1.

Table 1. Comparison of different wind turbine emulation (*WTE*) configurations

Reference	**Prime mover**	**Used converter**	**Required measurements**	**Model knowledge**	
				Controller	**Observer**
[20]	*IM* Motor	*3* Phase *IGBT* Inverter	• Torque • Speed	Required (*PI* Controller)	No observer used
[17]	*PMSM* Motor	3 Phase *IGBT* Inverter	• Position • Current (2)	Required	No observer used
[26]	*DC* Motor	Thyristorized bidirectional *AC/DC* interfaced	• Current • Torque • Speed	Required (*PI* Controller)	No observer used
[15]	*DC* Motor	*DC-DC* Converter	• Speed • Current	Required (*PI* Controller)	No observer used
[13]	*DC* Motor	*DC-DC* Converter	• Speed • Current	Required (*PI* Controller)	No observer used
[5]	*DC* Motor	*DC-DC* Buck converter	Not mentioned	Not mentioned	No observer used
This work	*DC* Motor	*DC-DC* Boost Converter	• Voltage • Current	Not Required (Fuzzy Logic Controller)	Required (*STA-SMO* observer)

This article includes a detailed description for the construction of a low cost wind turbine emulator. Each part has been experimentally validated. *Dspace card* and *ControlDesk* software were used for the implementation phase. The experimental tests start firstly, by validating the

proposed second-order sliding-mode speed observer based on super-twisting algorithm under different conditions. Secondly, the wind turbine characteristics has been extracted experimentally in open loop mode for different wind speed values and by considering two different power coefficient models. Finally, the wind turbine emulator has been tested in closed loop mode by using a fuzzy logic controller and under random step wind speed profile. The obtained results show: a high estimation performance of the proposed speed observer, a good emulation of the wind turbine characteristics in open loop mode and an accurate reaction as a real wind turbine in the closed loop mode.

II. WIND TURBINE MODEL AND DESCRIPTION

The power of the wind is defined by:

$$p_v = \frac{(\rho . A . {v_w}^3)}{2} \tag{1}$$

Where ρ is the air density, A is the circular area, v_w is the wind speed.

The mechanical power produced by the turbine can be expressed by:

$$p_m = \frac{1}{2} C_p(\lambda, \beta) . \rho . A . {v_w}^3 \tag{2}$$

$$\lambda = \frac{\Omega_m^G R}{v_w} \tag{3}$$

Where C_p represents the power coefficient, it depending on the pitch angle β and the tip speed ratio λ, Ω_m^G is the turbine rotor speed and R is the turbine radius.

For any given wind turbine manufactured, there is a specific characteristic of the power coefficient C_p. The expressions (4), (5) and (6) represent the main power coefficient C_p models proposed in [3][7][23][28][29] and used in literature.

$$\begin{cases} C_{p1}(\lambda, \beta) = C_1 \left(\frac{C_2}{\gamma} - C_3 . \beta - C_4 \right) e^{\frac{-C_5}{\gamma}} + C_6 . \lambda \\ C_1 = 0.5176, C_2 = 116, C_3 = 0.4, C_4 = 5, C_5 = 21, C_6 = 0.0068 \end{cases} \tag{4}$$

$$C_{p2}(\lambda) = (1.12\lambda - 2.8) e^{-0.38\lambda} \tag{5}$$

$$C_{p3}(\lambda, \beta) = 0.22 \left(\frac{116}{\gamma} - 0.4\beta - 5 \right) e^{\frac{-12.5}{\gamma}} \tag{6}$$

Where $\frac{1}{\gamma} = \frac{1}{\lambda + 0.08\beta} - \frac{0.035}{\beta^3 + 1}$.

Figures (1.a), (1.b) and (1.c) represent the characteristics of the power coefficient C_p as function of the tip speed ratio λ for the models (4), (5) and (6).

This study is mainly devoted to fixed-pitch angle wind turbines [27]; the pitch angle in equation (4) and (6) was set to zero. This does not mean that we cannot take it as a variable input in the case of variable pitch angle wind turbines.

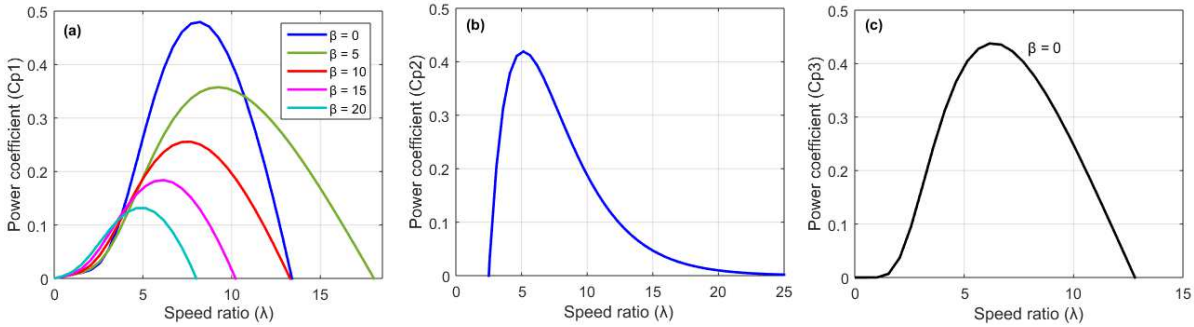

Fig.1. Power coefficient characteristics **a.** Power coefficient as function of tip-speed ratio for different pitch angle (Model (4)) **b.** Power coefficient as function of tip-speed ratio for fixed pitch angle wind turbine (Model (5)) **c.** Power coefficient as function of tip-speed ratio for the Model (6) with $\beta = 0$.

III. PERMANENT MAGNET SYNCHRONOUS GENERATOR (*PMSG*)

The coupled generator to the prime mover is a permanent-magnet synchronous generator (*PMSG*) whose model is given as follows:

The *d-q* stator voltage equations of this generator are given by the following expressions:

$$\begin{cases} V_{ds} = R_s I_{ds} + L_d \dot{I}_{ds} - \omega_r \psi_{qs} \\ V_{qs} = R_s I_{qs} + L_q \dot{I}_{qs} + \omega_r \psi_{ds} \\ \psi_{ds} = L_d I_{ds} + \psi_0 \\ \psi_{qs} = L_q I_{qs} \end{cases} \quad (7)$$

The differential equations of the *PMSG* can be obtained as follow:

$$\begin{cases} L_d \dot{I}_{ds} = V_{ds} - R_s I_{ds} + \omega_r L_q I_{qs} \\ L_q \dot{I}_{qs} = V_{qs} - R_s I_{qs} - \omega_r L_d I_{ds} - \psi_0 \omega_r \end{cases} \quad (8)$$

The electromagnetic torque is represented by:

$$T_{em}^G = \frac{3}{2} p\left[(L_d - L_q) I_{ds} I_{qs} + \psi_0 I_{qs}\right] \quad (9)$$

The *PMSG* is assumed to be wound-rotor, then $L_d = L_q$, and the expression of the electromagnetic torque in the rotor can be described as follow:

$$T_{em}^G = \frac{3}{2} p \psi_0 I_{qs} \quad (10)$$

Where L_d, L_q are the inductances of the generator on the q and d axis, R_s is the stator resistance, ψ_0 is the permanent magnetic flux, ω_r is the the electrical rotating speed of the PMSG which is given by $\omega_r = p.\Omega_m^G$ and p is the number of pole pairs.

IV. STUDIED WIND TURBINE EMULATOR

The designed wind turbine emulator is shown in Figure (2). Its consists of a *DC* power source, a *DC-DC* boost converter and a permanent magnets *DC* motor connected mechanically to the generator. In the wind turbine model, we have considered the three power coefficient equations (4), (5) and (6) in order to produce accurate dynamic characteristics as a real wind turbine. This latter will allows the user a flexible adaptation to the coupled generator type by selecting the appropriate C_p. The wind turbine inputs are the wind speed profile, the pitch angle and the rotational speed.

Sensorless control is one of the most important challenges in motor drives. The use of speed and position sensors in a system drive increase greatly the cost and volume of the control scheme. Adding to that, in the case of harsh working conditions, the use of such mechanical sensors will affect negatively the robustness and reliability of the system. In some cases, access to the motor shaft for installing a speed sensor is not possible. The cheapest and safest solution is the use of an observer or estimator. In this work, we propose a super-twisting algorithm (*STA*) based second-order sliding-mode (*SOSM*) observer for estimating the shaft speed of direct-current (*DC)* motors. The proposed *STA-SM* observer allows estimating the shaft speed only using a voltage and current sensor and without chattering problem.

The following sections focus particularly on the design of a robust rotational speed observer and an optimal fuzzy logic current controller.

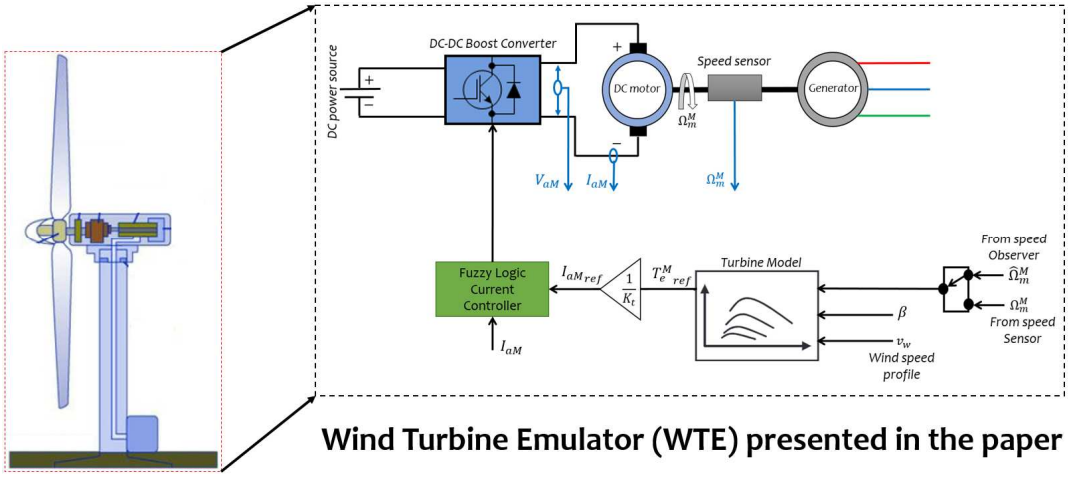

Fig.2. Studied wind turbine emulator (*WTE*) in this paper.

1. Second-order sliding-mode observer based on Super twisting algorithm

1.1. Mathematical model of a direct-current motor

The direct current motor mathematical model is expressed as follows [3]:

$$\begin{cases} V_{aM} = R_{aM} I_{aM} + L_{aM} \dot{I}_{aM} + e \\ T_e^M = K_t I_{aM} \\ e = K_e \Omega_m^M \\ T_e^M - T_L^M = J^M \dot{\Omega}_m^M + B_m . \Omega_m^M + T_f^M \end{cases} \quad (11)$$

Where R_{aM} is the armature winding resistance, L_{aM} is the armature self-inductance, I_{aM} is the motor armature current, V_{aM} is the applied voltage, e is the back *e.m.f* of the *DC* motor, K_e is the voltage constant, Ω_m^M is the angular speed, K_t is the torque constant, J^M is the moment of inertia, B_m is the viscous torque constant, T_f^M is the torque constant for rotational losses and T_e^M, T_L^M represent respectively the electromagnetic torque and load torque.

1.2. SMO-STA observer design

The super twisting algorithm (*STA*) aims to avoid the chattering problem of the conventional first-order *SMO*. The basic form of the super twisting algorithm in the presence of perturbation can be represented by the following differential inclusion [24][25]:

$$\begin{cases} \dot{\zeta}_1 = -\partial_1 |\bar{\zeta}_1|^{1/2} sign(\bar{\zeta}_1) + \zeta_2 + \varrho_1(\zeta_1, t) \\ \dot{\zeta}_2 = -\partial_2 sign(\bar{\zeta}_1) + \varrho_2(\zeta_2, t) \\ With\ (\bar{\zeta}_i = \hat{\zeta}_i - \zeta_i);\ (i = 1,2) \end{cases} \quad (12)$$

Where $\bar{\zeta}_i$ represents the error between the estimated values $\hat{\zeta}_i$ and the actual values ζ_i, ∂_1 and ∂_2 are gains to be designed and $\varrho_1(\zeta_1, t)$, $\varrho_2(\zeta_2, t)$ are the perturbation terms.

The perturbation terms of (12) are globally bounded by

$$|\varrho_1| \leq \vartheta_1 |\zeta_1|^{1/2}, |\varrho_2| \leq \vartheta_2 \quad (13)$$

For any ϑ_1, ϑ_2 positive constants (ϑ_1, $\vartheta_2 \geq 0$) and if the gains satisfy [25]:

$$\begin{cases} \partial_1 > 2\vartheta_1 \\ \partial_2 > \partial_1 \dfrac{5\vartheta_1\partial_1 + 6\vartheta_2 + 4(\vartheta_1 + {\vartheta_2}/{\partial_1})^2}{2(\partial_1 - 2\vartheta_1)} \end{cases} \quad (14)$$

Then the system will converge in finite time to the sliding surface. For the case, when $\varrho_2(\zeta_2, t) = 0$ [24], the gains ∂_1 and ∂_2 must satisfy $\partial_1 > 2\vartheta_1$, $\partial_2 > \partial_1 \frac{5\vartheta_1\partial_1 + 4{\vartheta_1}^2}{2(\partial_1 - 2\vartheta_1)}$.

The stability and finite time convergence of the perturbed system (8) are analyzed and verified using the following *Lyapunov* function [25]:

$$V(\zeta) = 2\partial_2|\zeta_1| + \frac{1}{2}\zeta_2^2 + \frac{1}{2}\left(\partial_1|\zeta_1|^{1/2}sign(\zeta_1) - \zeta_2\right)^2 \quad (15)$$

The time derivative of (15) can be rewetting as follows:

$$\dot{V} = \frac{1}{|\zeta_1|^{1/2}} z^T Q z + \frac{\varrho_1}{|\zeta_1|^{1/2}} q_1^T z + \varrho_2 q_2^T z \quad (16)$$

Where $q_1^T = \left[\left(2\partial_2 + \frac{\partial_1^2}{2}\right) \quad -\frac{\partial_1}{2}\right]$, $q_2^T = [-\partial_1 \quad 2]$ and $z^T = \left[|\zeta_1|^{1/2}sign(\zeta_1) \ , \ \zeta_2\right]$.

By using the bounds on the perturbation terms in (13) it can be shown that

$$\dot{V} \leq -\frac{1}{|\zeta_1|^{1/2}} z^T \tilde{Q} z \quad (17)$$

Where

$$\tilde{Q} = \frac{\partial_1}{2}\begin{bmatrix} 2\partial_2 + \partial_1^2 - \left(\frac{4\partial_2}{\partial_1} + \partial_1\right)\vartheta_1 - 2\vartheta_2 & \star \\ -\left(\partial_1 + 2\vartheta_1 + \frac{2\vartheta_2}{\partial_1}\right) & 1 \end{bmatrix}$$

Where $\star$ is used to indicate a symmetric element.

If $\tilde{Q} > 0$, then $\dot{V}$ is negative definite. It can be seen that $\tilde{Q} > 0$ if the gains are selected as (14).

First, to estimate the shaft speed, an armature current observer was designed using a sliding second-order *SMO* based on super twisting algorithm. Considering the estimated armature current $\hat{I}_{aM}$ as a state variable, by substituting $\zeta_1 = \hat{I}_{aM}$ into system *(12)*. The expression of *(12)* becomes as follows:

$$\dot{\hat{I}}_{aM} = -\partial_1|\bar{I}_{aM}|^{1/2}sign(\bar{I}_{aM}) - \int \partial_2 sign(\bar{I}_{aM})dt + \varrho_1(\hat{I}_{aM}, t), \quad (18)$$

$$With: \ (\bar{I}_{aM} = \hat{I}_{aM} - I_{aM})$$

The perturbation term $\varrho_1(\hat{I}_{aM}, t)$ is given as follows:

$$\varrho_1(\hat{I}_{aM}, t) = \frac{V_{aM}}{L_{aM}} - \frac{R_{aM}\hat{I}_{aM}}{L_{aM}} \quad (19)$$

By replacing the perturbation term ϱ_1 in (12*)* by $\frac{V_{aM}}{L_{aM}} - \frac{R_{aM}\hat{I}_{aM}}{L_{aM}}$, the armature current observer can be formulated as:

$$\dot{\hat{I}}_{aM} = \frac{V_{aM}}{L_{aM}} - \frac{R_{aM}\hat{I}_{aM}}{L_{aM}} + \frac{1}{L_{aM}}\partial_1|\bar{I}_{aM}|^{1/2}sign(\bar{I}_{aM}) + \frac{1}{L_{aM}}\int \partial_2 sign(\bar{I}_{aM})dt \quad (20)$$

Substituting (19) into (13), when $\varrho_2(\zeta_2, t) = 0$ and by replacing ζ_1 by the estimated armature current $\hat{I}_{aM}$. Equation (9) can be expressed as:

$$\frac{V_{aM}}{L_{aM}} - \frac{R_{aM}\hat{I}_{aM}}{L_{aM}} - \vartheta_1 \left|\hat{I}_{aM}\right|^{1/2} \leq 0 \qquad (21)$$

The inequality (21) can be satisfied by selecting a large enough ϑ_1.

Subtracting $\dot{I}_{aM} = \frac{V_{aM}}{L_{aM}} - \frac{R_{aM}I_{aM}}{L_{aM}} - \frac{e}{L_{aM}}$ from (20), the state equation of the armature current is given as follows:

$$\dot{\tilde{I}}_{aM} = \dot{\hat{I}}_{aM} - \dot{I}_{aM} = \frac{R_{aM}}{L_{aM}}\left(\hat{I}_{aM} - I_{aM}\right) + \frac{1}{L_{aM}}\left[\partial_1 \left|\hat{I}_{aM} - I_{aM}\right|^{1/2} sign\left(\hat{I}_{aM} - I_{aM}\right) + \int \partial_2 sign\left(\hat{I}_{aM} - I_{aM}\right)dt + e\right] \qquad (22)$$

The estimated value converges to the actual value when the estimation error is on the sliding surface and the system is stable. Then, the equivalent control method can be used to obtain the estimated back *e.m.f* of the *DC* motor.

$$\hat{e} = -\partial_1 \left|\hat{I}_{aM} - I_{aM}\right|^{1/2} sign\left(\hat{I}_{aM} - I_{aM}\right) - \int \partial_2 sign\left(\hat{I}_{aM} - I_{aM}\right)dt \qquad (23)$$

Finally, the estimated shaft speed of the *DC* motor is obtained as follows:

$$\hat{\Omega}_m^M = {}^{\hat{e}}/_{K_e} = \frac{1}{K_e}\left(-\partial_1 |\bar{I}_{aM}|^{1/2} sign(\bar{I}_{aM}) - \int \partial_2 sign(\bar{I}_{aM})dt\right) \qquad (24)$$

- ***Stability analysis:***

Considering the following differential inclusion for the unperturbed case of the system (12):

$$\begin{cases} \dot{\zeta}_1 = -\partial_1 |\bar{\zeta}_1|^{1/2} sign(\bar{\zeta}_1) + \zeta_2 \\ \dot{\zeta}_2 = -\partial_2 sign(\bar{\zeta}_1) \end{cases} \qquad (25)$$

Let the *Lyapunov* function be:

$$v = \partial_2 |\bar{\zeta}_1| + \frac{1}{2}{\zeta_2}^2 \qquad (26)$$

The derivative of the *Lyapunov* function () gives:

$$\dot{v} = \partial_2 sign(\bar{\zeta}_1)\left(\zeta_2 - \partial_1 |\bar{\zeta}_1|^{1/2} sign(\bar{\zeta}_1)\right) + \zeta_2\left(-\partial_2 sign(\bar{\zeta}_1)\right)$$

$$\dot{v} = -\partial_1 \partial_2 |\bar{\zeta}_1|^{1/2} < 0 \qquad (27)$$

The derivative of the selected *Lyapunov* function (26) is negative. Then the error system is asymptotically stable.

2. Fuzzy logic armature current controller design

The wind turbine mathematical model generates the reference armature current $I_{aM_{ref}}$ that correspond to the set wind speed and pitch angle [15]. The generated armature current reference $I_{aM_{ref}}$ is then compared to the instantaneous measured armature current I_{aM}. The error between the two quantities is used as input to the proposed controller. The armature current value can be adjusted by acting on the duty cycle α. The *Fuzzy Logic Controller* is selected for this application. In most of fuzzy logic control applications the generalized structure of this controller can be represented as shown in Figure (3). It's composed of three parts: *fuzzification, inference engine* and *defuzzification.*

- *Fuzzification*

Let $\varepsilon(k) = I_{aM_{ref}}(k) - I_{aM}(k)$ be the error between the armature current measured instantly at the sampling instant (k) and the reference armature current generated by the wind turbine model $I_{aM_{ref}}$. The variable $\varepsilon(k)$ is selected as the fuzzy system input and the change step of duty cycle $\Delta\alpha(k)$ is calculated as the output depending on the amount of the error between $I_{aM_{ref}}(k)$ and $I_{aM}(k)$.

The duty cycle α that will control the *DC-DC* boost converter is calculated using the following equation:

$$\alpha(k) = \alpha(k-1) + \Delta\alpha(k) \qquad (28)$$

The error variable $\varepsilon(k)$ provides to the fuzzy controller two main informations, the first one indicate the sign of the input signal, that is to say if the armature current is below or above its reference $I_{aM_{ref}}$, and the second one is to indicate the amount of the error, the task here is to identify the appropriate value of the duty cycle change step $\Delta\alpha(k)$ in order to keep the error between $I_{aM_{ref}}$ and I_{aM} equal to zero.

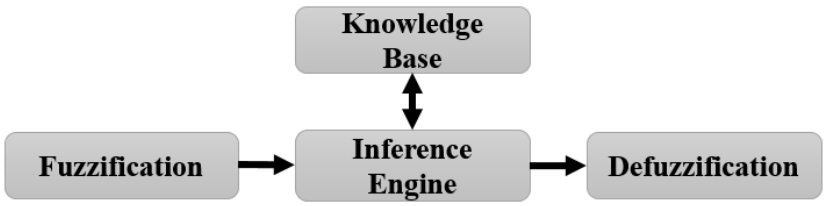

Fig.3. Basic illustration of the Fuzzy logic controller.

The values of membership functions are assigned to the linguistic variables using five fuzzy subsets for the input error variable $\varepsilon(k)$: N_{iB}, N_{iS}, Z_e, P_{i_S} and P_{i_B} and five fuzzy subsets x_{i_1}, x_{i_2}, Z_e, y_{i_1} and y_{i_2} for the output fuzzy variable $\Delta\alpha(k)$. Triangular symmetrical memberships functions forms are selected for the input and output variables as shown in Figures (4) and (5).

- *Inference engine*

The fuzzy logic generator consists of set of "***If-Then***" fuzzy rules, the five rules was designed and represented as below:

- ***If*** $\varepsilon(k)$ is N_{iB} ***Then*** $\Delta\alpha(k)$ is x_{i_2}
- ***If*** $\varepsilon(k)$ is N_{iS} ***Then*** $\Delta\alpha(k)$ is x_{i_1}
- ***If*** $\varepsilon(k)$ is Z_e ***Then*** $\Delta\alpha(k)$ is Z_e
- ***If*** $\varepsilon(k)$ is P_{i_S} ***Then*** $\Delta\alpha(k)$ is y_{i_1}
- ***If*** $\varepsilon(k)$ is P_{i_B} ***Then*** $\Delta\alpha(k)$ is y_{i_2}

As a fuzzy inference method, *Mamdani* method is used with *Max-Min* operation fuzzy combination law.

- *Defuzzification*

The output of fuzzy controller is a fuzzy subset of control. *Nonfuzzy* values are required for the control that can be done by using a *defuzzification* stage. The *defuzzification* will allows transforming and converting the fuzzy results from the fuzzy system into crisp values [3]. For this *Mamdani*-style inference the *defuzzification* is performed using the centroid method (or the center of gravity) method. The fuzzy rules outputs are combined together using centroid according to [3]:

$$y = \frac{\Sigma_{j=1}^{n} y_j \mu(y_j)}{\Sigma_{j=1}^{n} \mu(y_j)} \qquad (29)$$

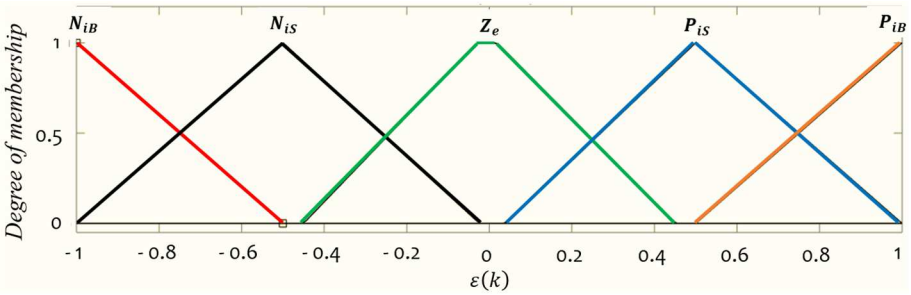

Fig.4. Membership functions for the input variable ($\varepsilon(k) = I_{aM_{ref}}(k) - I_{aM}(k)$).

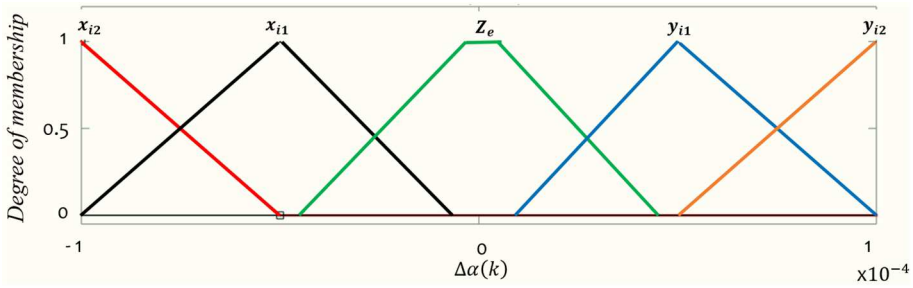

Fig.5. Membership functions for the output variable ($\Delta\alpha(k)$).

V. HARDWARE IMPLEMENTATION, RESULTS AND DISCUSSION

Figures (6) and (14) show the realized test bench for emulating the nonlinear wind turbine behavior. The performance of the speed observer, the open loop wind turbine emulator and the closed loop based on fuzzy logic controller (*FLC*) have been experimentally tested under different conditions. First, several tests were made to check the speed estimation performance of the proposed second-order sliding-mode observer based on super twisting algorithm. Secondly, the nonlinear wind turbine characteristics has been extracted experimentally in open loop mode for different wind speed values, and by considering two models of the power coefficient as an example. Finally, the closed loop wind turbine emulator operation was performed using the fuzzy logic technique.

- **Speed observer validation**

Figure (7) illustrates the used experimental setup for validating the presented *SMO-STA* observer. The test bench consists of a *DC* power source, a *DC-DC* boost converter and a direct-current motor connected to a mechanical load (generator connected to a 3 phase variable resistive load) in order to simulate the external load disturbance. The second-order sliding-mode super twisting observer was implemented on *Dspace* card. Three sensors were used during the experimental tests, an armature voltage and current sensors as input information to the speed observer, and a mechanical speed sensor to provide the real-time speed measurement and then making a comparison with the estimated value. The *PWM* signal switching frequency of the *DC-DC* boost converter was fixed at *10 KHz*.

Figure (8) shows the developed screen in *ControlDesk* software for the speed observer experiments. Figures (9) and (10) show the performances of the proposed second-order sliding-mode super twisting speed observer. In the first test, we have considered an increasing and decreasing ramp profile, the obtained results show a good estimation of the rotational speed information during transient and steady state regime. In a second test, we evaluate the estimation performances of the *SMO-STA* in the most difficult working conditions, a random

profile was considered, the results show a high estimation accuracy. As we can notice, in both tests, the maximum speed estimation error is around $\pm 1\ rad/s$.

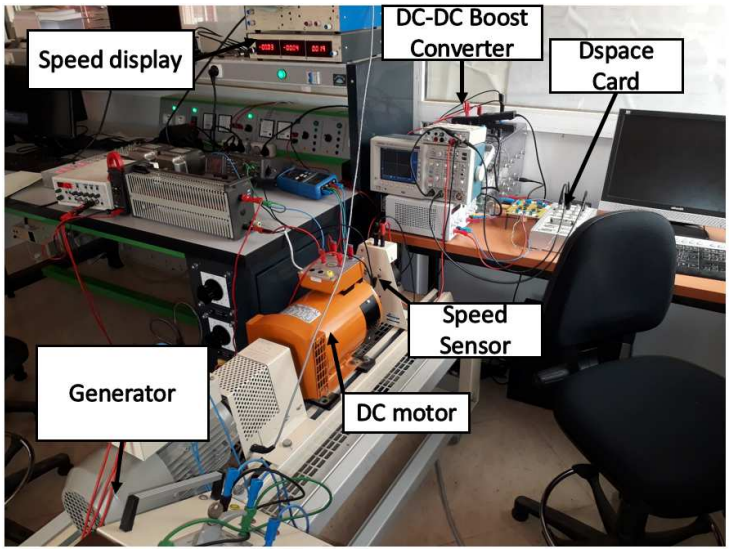

Fig.6. Experimental setup of the realized wind turbine emulator (*WTE*).

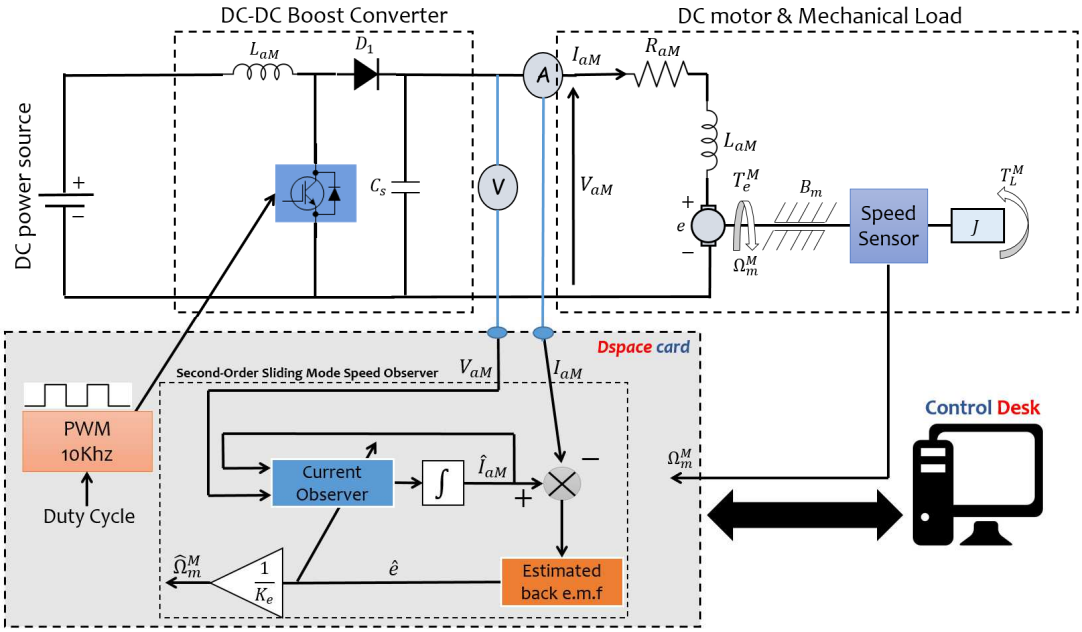

Fig.7 Experimental setup for validating the *SMO-STA* observer.

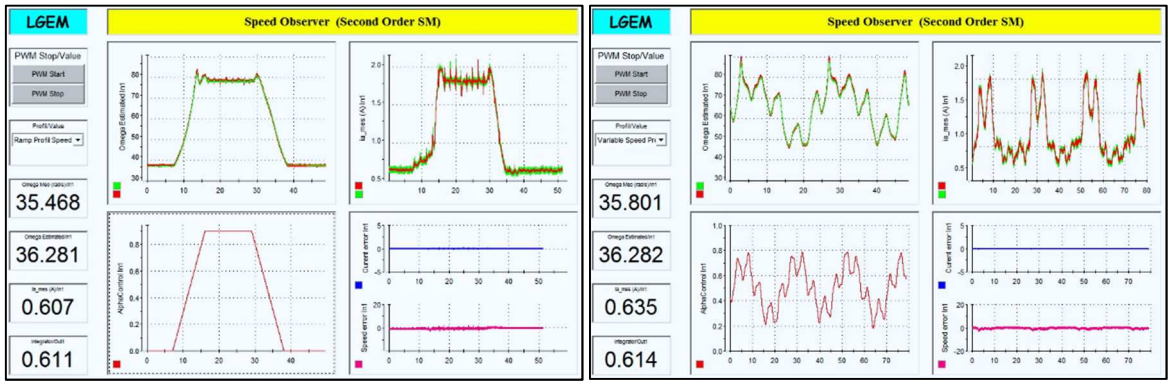

Fig.8 *ControlDesk* Screen of the speed observer experiments graphical interface.

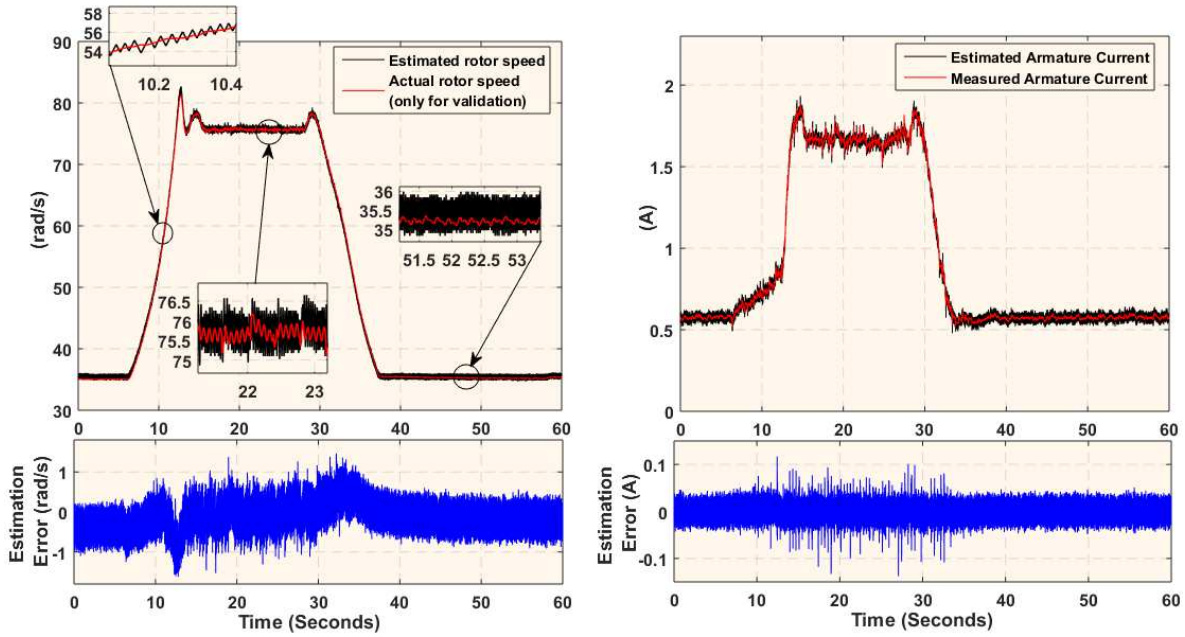

Fig.9 Experimental estimation performance under increasing and decreasing rotational speed profile.

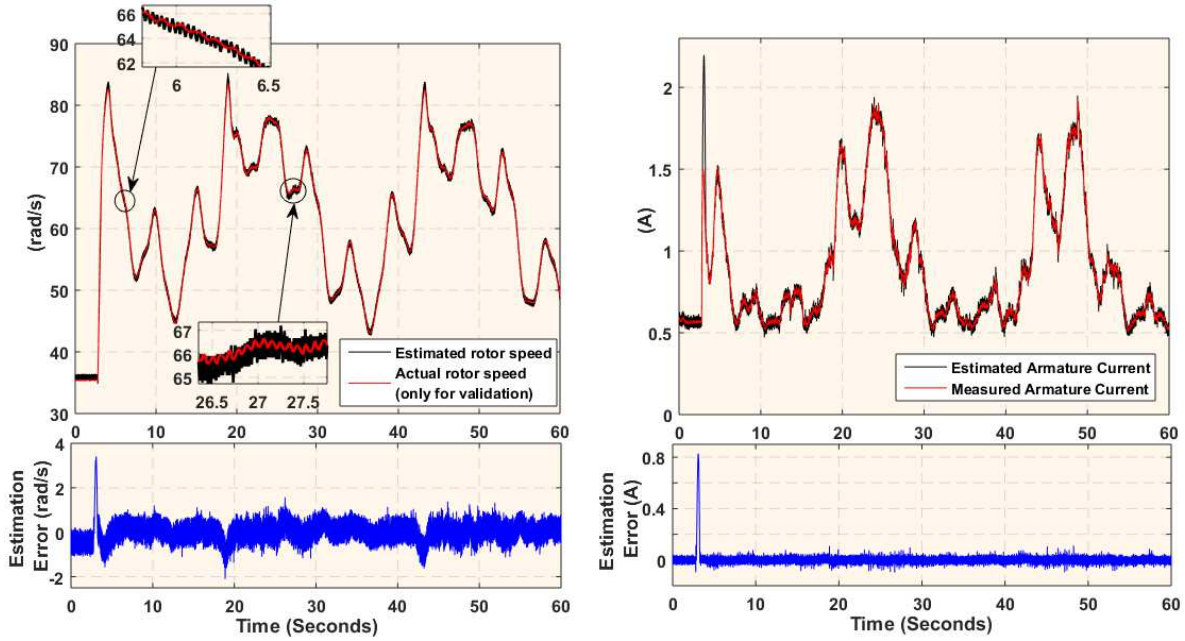

Fig.10 Experimental estimation performance under random rotational speed profile.

- **Open loop emulation of the turbine power curves**

In the open loop mode, the duty cycle of the *DC-DC* boost converter has been changed from *0* to *0.9* for each fixed wind speed value and for each power coefficient equation. The task here consists of extracting the characteristics of the turbine mechanical power as function of the turbine rotor speed. We have took a wind speed variation ranging from *4.5m/s* to *7m/s* as an example. Figure (11) shows the developed and the used graphical interface on *ControlDesk* environment to select the mode and desired power coefficient model. Figure (12) depicts the

obtained wind turbine characteristics by selecting the model of the power coefficient C_{p1} and Figure (13) depicts the wind turbine characteristics in the case of selecting the model of the power coefficient C_{p3}. From the obtained results, it can be observed that the designed *WTE* is able to produce and simulate the nonlinear behavior of a wind turbine whatever its power coefficient characteristic.

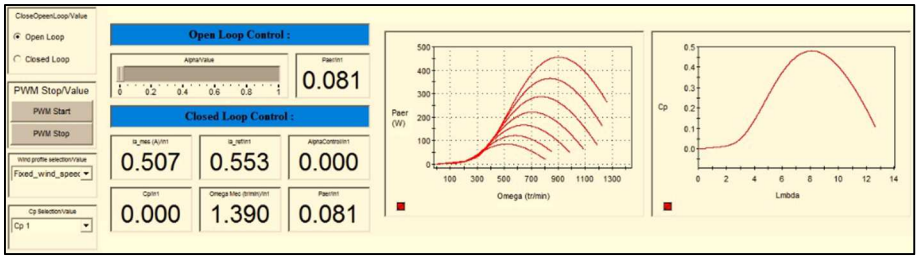

Fig.11 Graphical interface for the developed *WTE*.

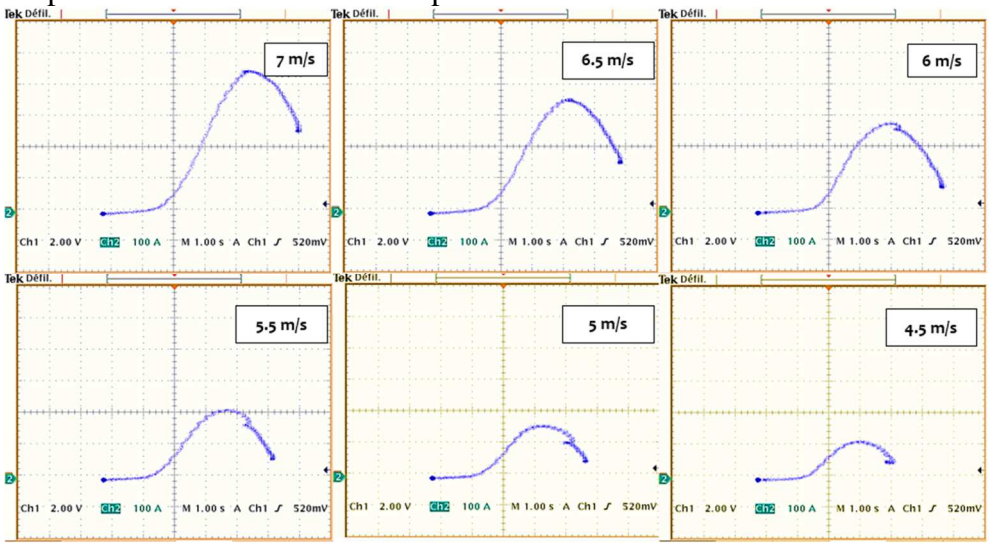

Fig.12 Open loop extraction of the wind turbine characteristics when selecting the first power coefficient model (C_{p1}).

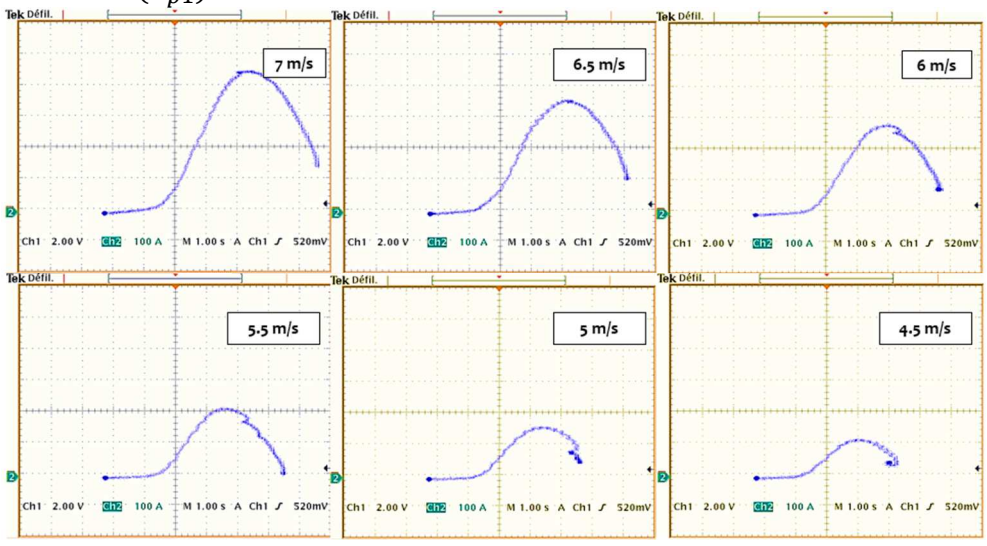

Fig.13 Open loop extraction of the wind turbine characteristics when selecting the third power coefficient model (C_{p3}).

- **Closed loop operation of the emulator**

Figure (14) shows the final configuration of the wind turbine emulator (*WTE)* working in closed loop mode used to simulate the nonlinear behaviors of a real wind turbine. In order to check and evaluate the *WTE* during dynamic and steady state regime, a step wind profile has been selected for this purpose. The wind speed has been changed from *5m/s*, *4m/s*, *6m/s*, *4.5m/s* to *5.5m/s* as shown in Figure 15.a. Figure .15b shows the generated duty cycle ($\alpha(k)$) of the *DC-DC* boost converter using the designed fuzzy logic controller (*FLC*), as we can see, no perturbation or noisy are presented on the command signal. Figure 15.d shows a good tracking of the generated reference armature current by the wind turbine mathematical model that corresponds to each set wind speed value. Figure 15.c shows the experimental *WTE* evolution on the theoretical mechanical turbine power/turbine rotor speed plane. It can be observed that the developed emulator reacts as a real wind turbine.

Figure (16) shows an explanation of the wind turbine emulator operation, Figure (16.a) represents the variation of the mechanical power and Figure (16.b) shows the variation of the shaft rotational speed of the prime mover. Taking as an example a sudden variation of the wind speed (from *4m/s* to *6m/s*). P_1 represents the operating point of the emulator at *4m/s* on the dotted brown curve, when applying a wind speed variation equal to *6m/s*, we can notice that our emulator (the green line) moves towards the characteristic which corresponds to *6m/s* (P_2) (the dotted black curve) then it stabilizes at point P_3. The operating points P_1 and P_3 depend on the connected load with the generator, this could be another points on each wind speed characteristic if we change load value.

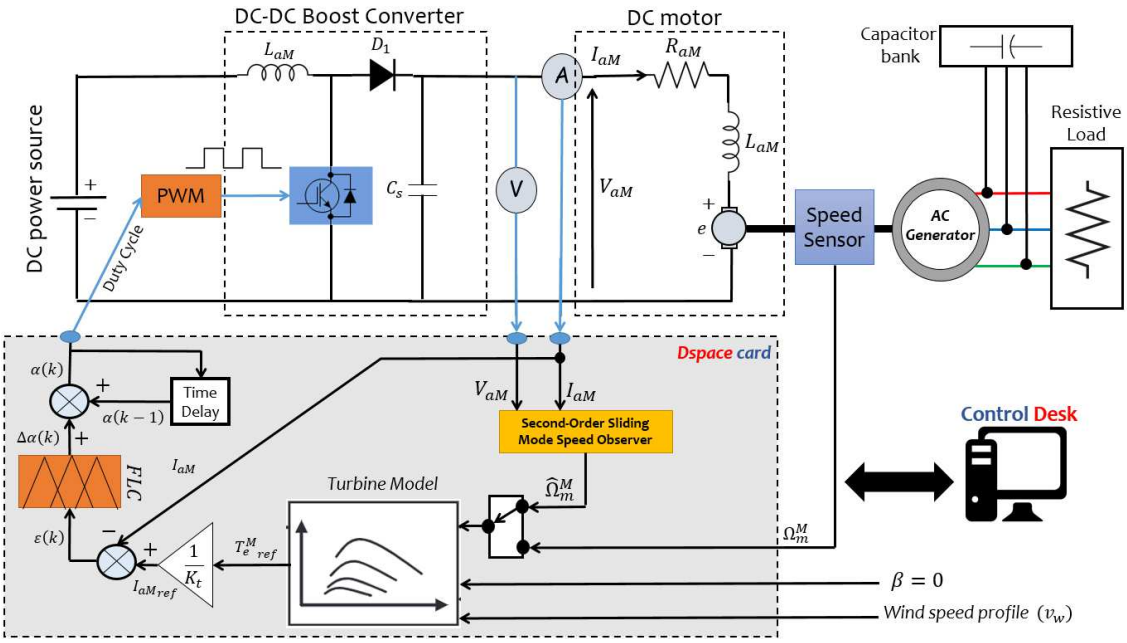

Fig.14. Designed sensorless wind turbine emulator (*WTE*) working in closed loop mode.

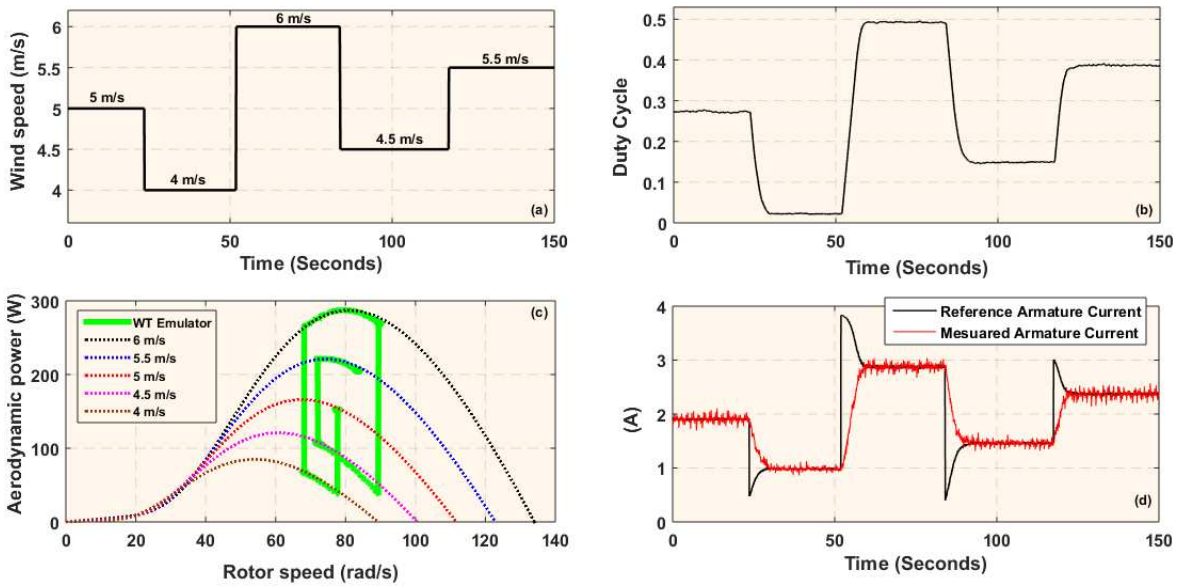

Fig.15. Experimental wind turbine emulation results, **a.** Applied step wind speed profile, **b.** Generated duty cycle using the proposed fuzzy logic controller (*FLC*), **c.** *WTE* evolution in the mechanical power/rotor speed plane, **d.** variation of the reference and the measured armature current of the *DC* motor.

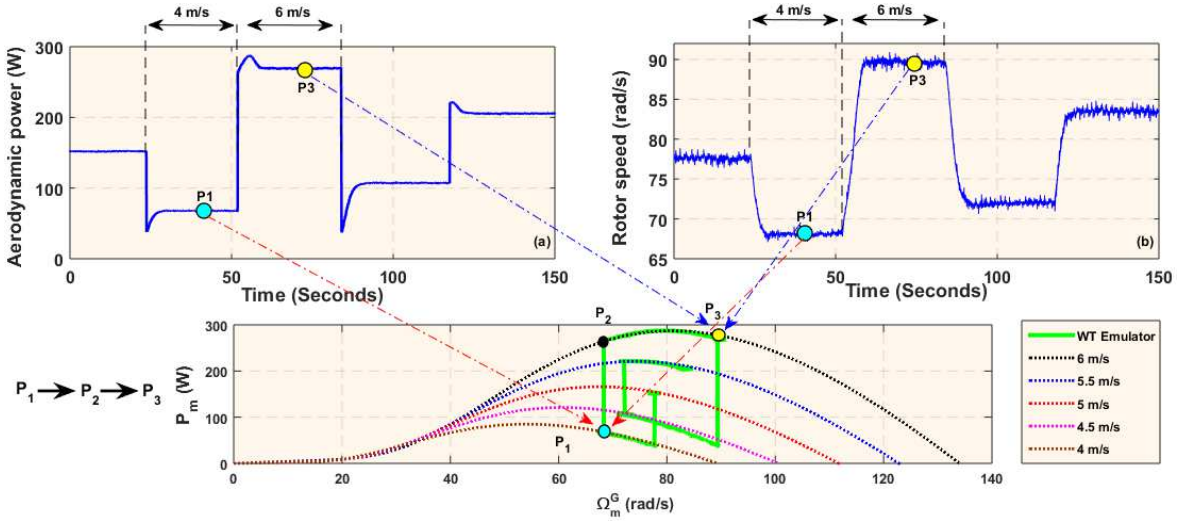

Fig.16. Explanation of the *WTE* operation **a.** Variation of the mechanical power**, b.** Variation of the rotational speed

VI. CONCLUSIONS

This paper deals with the design and realization of a low cost wind turbine emulator. The wind turbine model as well as the different power coefficient models were implemented on *DSpace* card. The shaft rotational speed information of the prime mover has been estimated using a second order sliding mode observer (*SMO-STA*) and using the armature voltage and the armature current as input information instead of using a mechanical speed sensor. The closed loop operation of the developed wind turbine emulator is ensured here using the fuzzy logic technique. The proposed controller does not need knowledge of exact system mathematical model and it's straightforward to implement. The obtained results have shown: high estimation

performance during dynamic and steady state regime for the speed observer tests, an accurate reproduction of the nonlinear behavior and the nonlinear characteristics of the wind turbines for the open loop tests and a reaction as a real wind turbine for the closed loop mode.

Acknowledgment. This research was supported by the National Center for Scientific and Technical Research (CNRST) of Morocco and the Embassy of France in Morocco.

REFERENCES

[1] Ramanath, Anushree, et al. "An Extremely Low-Cost Wind Emulator." IECON 2018-44th Annual Conference of the IEEE Industrial Electronics Society. IEEE, 2018.

[2] Dolan, Dale, and P. W. Lehn. Real-time wind turbine emulator suitable for power quality and dynamic control studies. University of Toronto, 2005.

[3] Soufyane, Benzaouia, et al. "A Comparative Investigation and Evaluation of Maximum Power Point Tracking Algorithms Applied to Wind Electric Water Pumping System." International Conference on Electronic Engineering and Renewable Energy. Springer, Singapore, 2018.

[4] Hardy, Trevor, and Ward Jewell. "Emulation of a 1.5 Mw wind turbine with a dc motor." 2011 IEEE Power and Energy Society General Meeting. IEEE, 2011.

[5] Moussa, Intissar, Adel Bouallegue, and Adel Khedher. "New wind turbine emulator based on DC machine: hardware implementation using FPGA board for an open-loop operation." IET Circuits, Devices & Systems 13.6 (2019): 896-902.

[6] Tammaruckwattana, Sirichai, and Kazuhiro Ohyama. "Experimental Verification of Variable speed wind power generation system using permanent magnet synchronous generator by Wind Turbine Emulator." IECON 2012-38th Annual Conference on IEEE Industrial Electronics Society. IEEE, 2012.

[7] Martinez, Fernando, L. Carlos Herrero, and Santiago de Pablo. "Open loop wind turbine emulator." Renewable Energy 63 (2014): 212-221.

[8] Monfared, Mohammad, Hossein Madadi Kojabadi, and Hasan Rastegar. "Static and dynamic wind turbine simulator using a converter controlled dc motor." Renewable Energy 33.5 (2008): 906-913.

[9] Liu, Guangchen, Shengtie Wang, and Jike Zhang. "Design and realization of DC motor and drives based simulator for small wind turbine." 2010 Asia-Pacific Power and Energy Engineering Conference. IEEE, 2010.

[10] Battaiotto, P. E., R. J. Mantz, and P. F. Puleston. "A wind turbine emulator based on a dual DSP processor system." Control Engineering Practice 4.9 (1996): 1261-1266.

[11] Li, Weiwei, et al. "Research on wind turbine emulation based on DC motor." 2007 2nd IEEE Conference on Industrial Electronics and Applications. IEEE, 2007.

[12] Abdallah, M. E., and O. M. Arafa. "Design and control of one kilowatt DC motor-based wind turbine emulator." International Journal of Engineering Research 5.3 (2016): 185-189.

[13] Chen, Jian, et al. "Design of robust MPPT controller for grid-connected PMSG-Based wind turbine via perturbation observation based nonlinear adaptive control." Renewable energy 134 (2019): 478-495.

[14] Benaaouinate, L., et al. "Emulation of a Wind Turbine with a DC Motor controlled by Fuzzy Logic controller." vol 20 (2017): 97-101.

[15] Afghoul, Hamza, et al. "Design and real time implementation of sliding mode supervised fractional controller for wind energy conversion system under sever working conditions." Energy Conversion and Management 167 (2018): 91-101.

[16] Kouadria, S., et al. "Development of real time wind turbine emulator based on DC motor controlled by PI regulator." 2013 Eighth International Conference and Exhibition on Ecological Vehicles and Renewable Energies (EVER). IEEE, 2013.

[17] Abdallah, Mohamed E., et al. "Wind turbine emulation using permanent magnet synchronous motor." Journal of Electrical Systems and Information Technology 5.2 (2018): 121-134.

[18] Hu, Weihao, et al. "Development of wind turbine simulator for wind energy conversion systems based on permanent magnet synchronous motor." 2008 International Conference on Electrical Machines and Systems. IEEE, 2008.

[19] Yan, Jianhu, Yi Feng, and Jianning Dong. "Study on dynamic characteristic of wind turbine emulator based on PMSM." Renewable Energy 97 (2016): 731-736.

[20] Kojabadi, Hossein Madadi, Liuchen Chang, and Tobie Boutot. "Development of a novel wind turbine simulator for wind energy conversion systems using an inverter-controlled induction motor." IEEE Transactions on Energy conversion 19.3 (2004): 547-552.

[21] Castelló, Jaime, José M. Espí, and Rafael García-Gil. "Development details and performance assessment of a wind turbine emulator." Renewable energy 86 (2016): 848-857.

[22] Neammanee, Bunlung, Somporn Sirisumrannukul, and Somchai Chatratana. "Development of a wind turbine simulator for wind generator testing." International Energy Journal 8.1 (2007).

[23] Xia, Yuanye, Khaled H. Ahmed, and Barry W. Williams. "Wind turbine power coefficient analysis of a new maximum power point tracking technique." IEEE transactions on industrial electronics 60.3 (2012): 1122-1132.

[24] Liang, Donglai, Jian Li, and Ronghai Qu. "Sensorless control of permanent magnet synchronous machine based on second-order sliding-mode observer with online resistance estimation." IEEE transactions on industry applications 53.4 (2017): 3672-3682.

[25] Moreno, Jaime A., and Marisol Osorio. "A Lyapunov approach to second-order sliding mode controllers and observers." 2008 47th IEEE conference on decision and control. IEEE, 2008.

[26] Bhowmik, Shibashis, Rene Spee, and Johan HR Enslin. "Performance optimization for doubly fed wind power generation systems." IEEE Transactions on Industry Applications 35.4 (1999): 949-958.

[27] Sajadi, Amirhossein, et al. "An emulator for fixed pitch wind turbine studies." Renewable Energy 87 (2016): 391-402.

[28] Daili, Yacine, et al. "Quantitative Feedback Theory design of robust MPPT controller for Small Wind Energy Conversion Systems: Design, analysis and experimental study." Sustainable Energy Technologies and Assessments 35 (2019): 308-320.

[29] Kumar, Ravinder, et al. "Maximum power point tracking in wind energy conversion system using radial basis function based neural network control strategy." Sustainable Energy Technologies and Assessments 36 (2019): 100533.